Optimized operation of the MTT EnerTwin in non-continuous or part load operation

Magdalena Maj

majmagdalena@wp.eu
Instituto Superior Técnico, Universidade de Lisboa, Portugal
November 2017

Abstract

The presented work was performed to study the micro-CHP performance in order to maximize its efficiency while complying with the heat demand. An optimal strategy had to be found between the reduced electrical efficiency and power at part load in comparison with the start/stop and standby losses during intermittent operation.
The work starts with a general study of the MTT's micro-CHP system and obtaining an overview of full load, part load, start/stop and standby powers. Experiments of the system were performed under various conditions, different electrical loads and various initial temperatures of the system. Calculations of the tests results are the electrical energy and thermal energy produced, and fuel consumed. In the work, three operating modes of the system were distinguished: start (heating up), steady state and stop (cooling down). Electrical, thermal and fuel energy were expressed by functions dependent on the load and operational time. Energy functions in different modes of the micro-CHP were used to build the numerical model of the system. Simulations of the model were performed for two different heat demand profiles. The numerical model made it possible to compare the efficiency of the system at full load and at part load and, therefore, to optimize the system's performance in these two operation modes. The conclusion is that it is more efficient to operate the system in full load in terms of economic benefits.

Keywords: micro-CHP, buffer vessel, part load, transient, optimization, numerical model

1. INTRODUCTION

Distributed energy resources (DER) are expected to play a significant role in the future of the electricity supply. The DER's concept embraces three subconcepts: distributed energy storage, distributed generation of electricity (DG) and load management, i.e. controllable energy loads. DG technology examples are micro-CHP, small wind turbines, photovoltaic systems and other small renewable energy sources, like biogas digesters. Drivers for DG have increased energy efficiency due to co-generation options and fewer line losses, fuel diversification and autonomy, environmental benefits like carbon emissions reduction by the use of RES and more efficient usage of fossil fuels, and reduced investment risk. Additionally, placing a generation close to demand is increasing the reliability of delivered electricity and quality of power. Micro-CHP can play a key role in supporting crucial policy objectives such as market liberalization, increasing shares of the electricity generation from renewable sources, mitigating climate change and magnifying energy savings [1].Countries like the Netherlands have a high investment potential for micro-CHP where most of the residential space heating and hot water comes from the conversion of natural gas in boilers.

The main barrier to adoption of micro-CHP is the high initial cost. Economic aspects of micro-CHP have been investigated by many researchers. According to [2], the typical micro-CHP system can cost about 500 $/kW and the generation cost can be 45 – 50 $/MWh. The operating costs can be reduced by the applied optimized profile of the micro-CHP operation with thermal energy storage. There are several impacts on the economic performance of the plant that is comprehensively discussed in [1]. The paperwork is based on the micro-CHP plant equipped with thermal energy storage and additional boiler. It is worth to point out the various schemes of applications with micro-CHP [3]. Micro-CHP can be coupled with a cooling unit or other heat or electrical power generation unit, such as fuel cells, heat pumps, renewable energy sources [4].

There are different definitions of micro-CHP or micro-cogeneration. According to the European Cogeneration Directive micro-CHP are all units with an electric capacity less than 50 kW [5]. Micro-CHP run usually to produce heat for space heating and hot water in the residential or commercial building and small industries. It can replace conventional boilers. Unlike boilers micro-CHP produce electricity together with heat at high efficiency, saving the same fuel, reducing greenhouse gas emissions and lowering electricity prices. Micro-CHP can operate in parallel to the electricity network, meaning consumers can still receive some electricity from the grid but produced electric energy can be exported to the grid. The system can also operate as a stand-alone unit.

The growth of micro-cogeneration was simulated by the generous government subsidies. Since the production of power for CHP installations is more efficient than in separate units, it is an instrument for some countries to meet the EU requirements. Cogeneration technology has been developed not only in numbers produced but also in sizes. First plants had a rated power of hundreds of MWe, evolving from hundreds of kilowatts down to 1kWe. The creation of a profitable micro-CHP application is possible in such countries as the Netherlands, where the price of electricity and natural gas on the energy basis is significant. The key target markets are such countries as UK, Germany, the Netherlands, Italy, France, Belgium, Ireland, and Denmark. In the UK, there is the widest range of CHP starting from 1 kWe to the largest units of 740 kWe [6].

In the EU CHP is widespread. Units of several hundred megawatts can be found in refining and chemical industry and in a relatively smaller number of large district heating applications. Micro-cogeneration is an option for the small-scale provision of heat and electricity in the residential and commercial sector.

Micro-CHP uses the following types of engine:

- Internal combustion engine (ICE), which already exists on the market
- External combustion engine, usually Stirling, Rankine cycle or steam engines
- Fuel cells, that are still in the development or demonstration stages.

Currently, the cogeneration technology on a small-scale base mostly adopted ICE. However, in the last decade, microturbine is significantly increasing its market shares. The rising success of MT is due to its perfect modularity and useful flexibility characteristics (especially when it is used in clusters). These features make MT suitable for a wide range of loads, applications and fuels. Additionally, in terms of CO and NOx emissions, MT performance in comparison with ICE is better in full load operation [7]. Therefore, micro-CHP with MT can be more often encountered for instance in urban areas, where there are specific environmental restrictions.

Traditionally, the term ‘cogeneration’ is associated with power generation from fossil fuels. However, other sources can be adapted to cogeneration, namely solar power, allowing for clean and high-performance solutions. An Interesting concept is combining renewable sources and fossil fuel micro-CHP, even though renewable sources provide intermitted energy generation. The flexibility of combining various scales CHP plant with volatile energy resources as wind power can increase overall efficiency and economic performance of the integrated equipment. Additionally, by adding PV source even higher performance can be reached [8]. Further advantages can be gained through the installation of reversible electrical heat pumps to balance the possible excess of electricity from renewable sources for cooling or heat generation. In any case, an interesting economic benefit is exposed by the possibility of selling the electricity excess to the grid with the feed-in tariff according to the environmental regulations.

Many authors evaluated the economic benefits of micro-CHP system. They pointed out that the feasibility of this technology strongly depends on the user’s heat and electricity demand, the fuel prices and the feed-in tariff, as well as on the appropriate sizing of the prime mover and the thermal storage system.

In [9] there is addressed the optimization of the micro-CHP for residential purposes installed in Italy and operating only during winter time. The system there is equipped with a prime mover fed by natural gas, a thermal energy storage, and an auxiliary boiler. Two heat demand-driven strategies of micro-CHP work were implemented in the paper in order to maximize the revenue of the system in comparison to the separate power generation. The first one assumes that the heat is produced by the prime mover to satisfy the user’s requirements and to fill up the TES in one-hour step. In the second strategy, there is the possibility of dumping part of the heat produced

by PM. To solve the problem two software's were used: Matlab and TRNSYS 17. In Matlab, there was created a code for the economic optimization while the commercial software TRNSYS was used to dynamically model the micro-CHP system. In the work, the hypothesis of PM working only in full load was reported. The operation in part load mode was not considered. The authors take into account incentives that depend on the amount of saved TOE by the micro-cogeneration system and discuss sensitivity analysis on the system with the incentives. Another Italian author [10] underlines the benefits of the cogeneration system for the efficiency increase in residential buildings in terms of the EU politics. The aim is to optimize the power plant design in order to minimize the daily power production costs and environmental impacts. In this case, the power plant is equipped with micro-CHP and an absorption chiller, both coupled with thermal storage unit applied to the residential household. The user's profile is considered for different seasons of the year. NPV calculation shows an economic advantage in short and long-term coupling the thermal energy storage with micro-CHP loop and in the cooling loop. However, this gain is not sufficient and it is greater for bigger micro-CHP. Modification of the thermal storage volume did not show a significant impact on the results. In terms of environmental protection, it states that around 7% of the primary energy can be saved in comparison to the district electricity production in Italy and in not more than 3% of CO2. Similar results are found when changing the volume of the TES. The study presents the optimum case for the larger cooling CHP (CCHP) unit with an adequate electric load [11]. The CHP plant operates as an island, meaning it is not connected to the grid and its design and operation maximize efficiency and minimize investment and marginal cost for the residential neighborhood application. For the purpose of the study, the hourly data about heat, electricity, and cooling were collected and scaled up to meet the requirements of the specific neighborhood. A multi-scale problem was solved using a temporal Lagrangean decomposition with a hybrid Lagrange multiplier updating method. Part load performance of the regenerative micro-CHP system of 100 kW fired with dual fuel natural gas – biomass for residential purposes was discussed in [12]. All the simulations of the part load performance of the plant were performed in Gate Cycle software. Apart from the thermos-economic simulation of the power plan with the different fuels ratio, the conclusion from the paperwork is that the heat demand driven operation is the most efficient. There has been an interesting study of sensitivity analysis in the design and operation of μCHP [1]. There are technical and economic uncertainties that may influence implementation of the micro-CHP on the market. Those uncertainties were applied to the impact analysis and evaluation of the framework to a defined case study system. The mathematical model with which the impacts of the system uncertainties were quantified consists of a micro-CHP unit as a prime mover with an auxiliary boiler, electricity storage, and thermal storage. Only the full load of the power plant operation was considered.

2. METHODOLOGY

We decided to test the system in a few set points: 20%, 40%, 60%, 80%, and 100% electrical load. An important parameter influencing the start behavior of the EnerTwin is the temperature of the system. MTT uses the temperature of the recuperator (labeled Tt_34, measured by a redundant sensor) as the reference temperature of the system. The recuperator reflects the heating state of the system due to its high heat capacity. Depending on this temperature, the starting condition of the system can be considered as cold, warm or hot. Cold start occurs when the temperature of the system is similar to the ambient temperature: the system's components have to be warmed up before delivering heat to the circulating water. This takes time and while the system heats up there is no hot water production. In a warm start, the system is already able to deliver some amount of heat to the water. During a hot start, the system is hot enough to deliver the maximum possible heat to the water almost instantly after starting. To account for the influence of the system temperature, several starts of the system, at various starting temperatures (Tt_34_0) were performed: 300 K, 450 K, 600 K, 750 K and 860 K.

Part load operation causes efficiency losses. Figure 1 presents the relations in steady state between the electric output and the electric efficiency on the first axis and overall efficiency on the second axis. The electric efficiency (also net efficiency) is calculated as the ratio between the electric power output and the fuel power input, while the overall efficiency is the ratio between the sum of the electric power output and heat power output and the fuel power input. The bigger dots on the plots of Figure 1 represent nominal

power at specific set points. Values in between them were estimated by the second-degree polynomial.

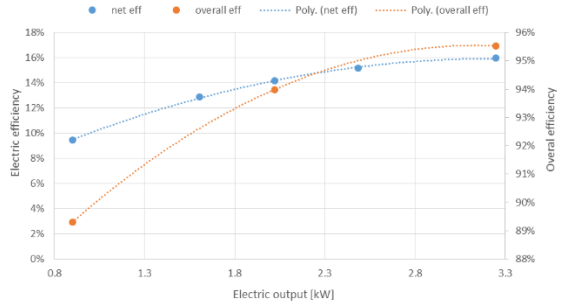

Figure 1 Part load efficiency

Since the system tends smoothly to steady state operation, we have to define the boundary between the transient and the steady state domain. We assumed that it should be possible to identify steady state conditions by observation of one or more parameters.

The processed data showed that thermal power could be a suitable parameter for defining the steady state. Thermal power is the result of multiplying water mass flow rate, water specific heat capacity and the temperature difference between the supply and return water temperature. The water mass flow rate meter exhibits many fluctuations, but these fluctuations have a repetitive pattern and can be easily averaged. The averaged power increases constantly until steady state. The time to reach steady state depends on the system temperature Tt_34_0 at the start. The warmer the system, the faster it reaches steady state. Experience showed that 1700 s is the minimum time for the system to reach steady state after a cold start. In all other tests, with higher initial Tt_34_0, the system was stable earlier. The considered time was increased from 1700 s to 2000 s to be sure that even in slightly different external conditions (i.e. different outside temperature), steady state was reached, even with a cold start.

Table 1 represents calculations of the electric, heat and fuel energy, 2000 s after the start of the tests, with various loads and initial recuperator temperatures. Energy values entail errors solely due to measurement devices' inaccuracies.

Table 1 Electric, thermal and fuel energy calculations 2000 s after starting the system for various loads and initial recuperator temperatures

SP [%]	Tt_34_0 [K]	E_el [kWh]	E_th [kWh]	E_f [kWh]
100	**599**	1.551	8.358	11.394
100	**864**	1.664	9.075	11.062
80	**600**	1.250	7.024	8.451
60	**444**	0.774	5.049	8.378
60	**571**	0.882	5.355	8.444
60	**754**	0.865	5.761	7.840
40	**451**	0.635	4.388	7.808
40	**628**	0.675	5.147	7.531
40	**738**	0.629	5.316	6.822
40	**872**	0.650	5.479	6.620
20	**444**	0.448	3.723	7.313
20	**762**	0.484	4.662	6.091

The next step was to obtain equations that allow calculating the electric, thermal and fuel energy for any value of SP and Tt_34_0.

The relation between variables cannot be linear since power code does not depend linearly on the electric power (Table 1). The difficulty was to find coefficients of Equation (1) to fit the set of data from the Table 4. Coefficients were received by the surface fitting to the energy values with the least squares method.

(1) $E_i = \beta_0 + \beta_1 * SP + \beta_2 * Tt_{34_0} + \beta_{11} * SP^2 + \beta_{22} {Tt_{34_0}}^2 + \beta_{12} * SP * Tt\_34\_0$

Where: i= {el, th, f}.

The results of the optimization are three sets of coefficients from the equation (1) that create three polynomial functions for the electric, thermal and fuel energy, respectively.

Produced thermal and electric power, and consumed fuel power during the steady state operation depends on the load. The higher the load, the higher value of the thermal, electric and fuel power. Cumulative thermal, electric or fuel energy produced is the integral of instantaneous thermal, electric or fuel power, respectively. Obviously, energy increases proportionally with the operational time. Therefore, each of

mentioned energies in steady state conditions can be expressed as a function of two independent variables: the set point and time.
When the speed of the engine is reduced to 0 rpm, the system is still hot enough to heat the circulating water and produce a further small amount of thermal energy.

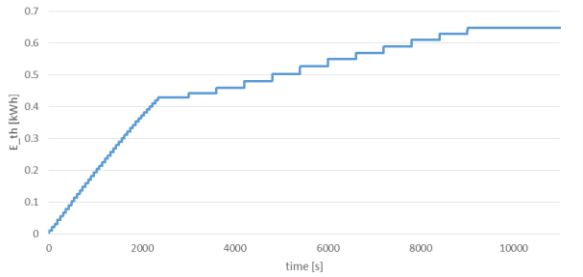

Figure 2 Accumulated heat production during cooling down of the system

Figure 2 represents the thermal energy produced in the first range of time (blue curve). The red dotted line is a linear approximation of the energy function. The relative error between the measured thermal energy and the fitted function is less than 1.5%.

There is still some electricity consumed by the electronic control and the pump during these two cooling down stages. The cabinet ventilator also works when the cabinet temperature is too high. From Figure 3 it is seen that the electric energy can be approximated by a second-degree polynomial.

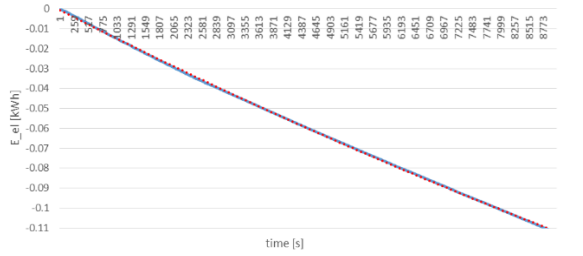

Figure 3 Electricity consumed during cooling down the system

The optimum operating profile needs to be determined to maximize the efficiency while complying with the heat demand. The concept of the optimization of the micro-CHP was to prove if it is worth to run the system in part load. Operation in part load and transient state, as start/stop is characterized by a smaller efficiency than the full load operation. When the system is equipped with a buffer vessel, its operation can be controlled by the temperature of the water inside the tank. As a result, this control implementation leads to forced start and stop of the system when the required buffer vessel temperature is reached. Operating the system in part load can prevent a number of stops. The numerical model should optimize the decision regarding how to operate the system, depending on the heat demand profile of the user and the TES size. The daily heat demand profile is discretized in time intervals bigger than 2000 s, which is the minimum time required for starting. The optimization algorithm has to make an optimal decision in every interval (every 2000 s) knowing the state of the system during the previous interval.

When there are several decisions to be made and some of them influence others, the general strategy should optimize the whole system. One way of doing this is to optimize subsystem inside a global optimization loop. The techniques used in dynamic programming consist of a combination of well-known algorithms: linear, integer, quadratic and nonlinear programming [13].

Figure 4 presents the flowchart of the system algorithm with its looping structure.

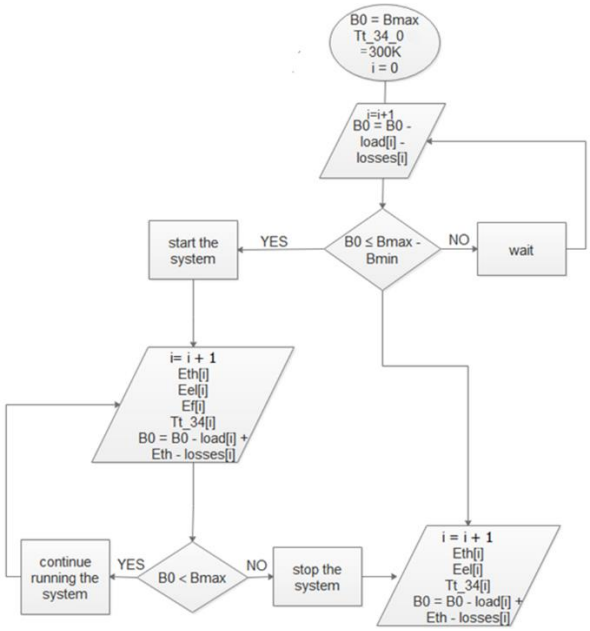

Figure 4 Flowchart of the system

To be able to optimize the operational control of the micro-CHP we chose the minimization of the overall running cost as the target function. The objective of the optimization is to minimize the overall cost-function described by:

(2) $Cost = \Sigma_i^{time\_steps}[- E\_el \ (p\_el\_buy + p\_el\_sub) + E\_f \ * p\_f]$

Where:
E_el – is the electric energy (in kWh) produced during time step *i*
p_el_buy – is the price of electricity (€/kWh) in Germany
p_el_sub – is the number of subsidies (€/kWh) for the production of electricity in micro-CHP
E_f – is the fuel energy (kWh) consumed during time step *i*
p_f – is the price (€/kWh) of the natural gas energy

3. RESULTS AND DISCUSSION

There are two different heat loads considered. One of them consists of the demand for the space heating and sanitary hot water, while the other covers the demand only for sanitary hot water, but for the larger scale. These load profiles are based on the profiles discussed in the section but they had to be scaled up (simply by multiplication). The values of powers in profiles had to be increased because the system has the too high capacity to comply with such a small demand and would have to operate significantly less frequently. The installation of the system for such demands would not be reasonable. However, the discussed heat demand profiles were still used to preserve the pattern of the heat demand profile. Furthermore, two different heat demand profiles (for the SHW and space heating and for SHW only) were used because the profile for the demand of sanitary hot water only contains some zero values, while the space heating demand is always greater than zero in the discussed profile. This can establish the behavior of the system in two different conditions. For each of the two heat demand profiles, the numerical model scheduled the operation of the system in two regimes. The first regime assumes operation only in a full load. There, the system can be in each interval only in two states: full load (SP = 100%) or inoperative (SP = 0). The other regime established in simulations for both types of heat demand profiles is when the system operates in a part load. Thus, its operation can have two status: operate in part load (SP < 100%) or inoperative (SP = 0).

a) Operation at full load

Figure 5 presents the outcome of the numerical model simulation for the heat demand profile covering space heating and heat for sanitary hot water. In this first simulation, it was assumed that the system could operate only at full load. Thus all the black columns on Figure 5 representing the set point (the load of the system) have the value of SP = 100%. In the code, it is reflected by the value of the variable Binary equal to True. The orange line represents the heat demand profile with the value of the required heat power in each interval on the secondary axis. As stated previously, the initial buffer vessel capacity is maximum. Therefore, according to the simulation, the system does not have to operate in the very first intervals, even though there is already heat demand. At the time, the capacity of the buffer vessel decreases, until the minimum capacity is reached and so the system should start operating. When the buffer vessel reaches its maximum capacity, the system should stop. The logic is repeated further on. In each interval, we calculate the electrical and heat energy production as well as the fuel energy consumption. The simulation produced two system operation states, represented in Figure 5 by the set point values (in this case 0 or 100). There are 11 bars, which means that the system should be started 11 times. The second output of the numerical model is that the values of the total electrical and the total fuel energy produced and consumed, respectively, during the 24 h. The total electrical energy and the total fuel energy is calculated as the sum of the electrical and fuel energy output in each interval, respectively. The third result of the simulation is the value of the objective function. The objective function that was minimized is the overall economic cost of the consumption of fuel, subtracting the overall economic cost of the extracted electrical energy.

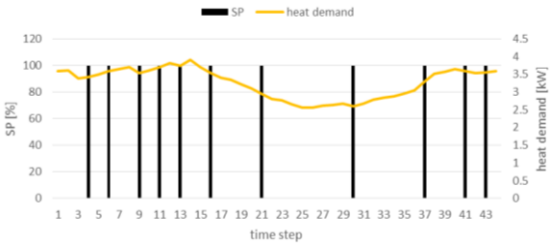

Figure 5 Simulated operating schedule of the system operations in full load with restriction to the total heat demand

b) Operation in part load

Figure 6 represents results of the simulation of the numerical model with the assumption that the system operates at part load to comply with the heat demand profile where there is the heat required for sanitary hot water and space heating. The black columns represent the value of the set

point that corresponds to the part load of the system. The number of bars corresponds to the number of starts of the system and it is higher (15 starts) than for the first simulation with a full load. The orange line represents the heat demand profile with its heat power values on the second vertical axis. Similarly, as in the first simulation system, at the initial time t = 0 the system is equipped with the buffer vessel at its maximum capacity. Hence, according to the simulation, in the initial intervals, the system does not need to operate and the set point SP is equal to 0. Only when the buffer vessel capacity drops below its minimum, due to occurred heat demand and the little influence of the heat losses (not including convection losses), the system starts operating. In Figure 6 one can see that the system operates more frequently when there is a higher heat power required. In each iteration, there is calculated electrical energy produced and fuel energy consumption and then summed up. As a result, there is the overall cost evaluated.

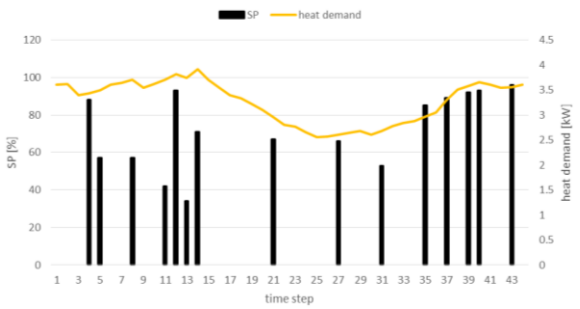

Figure 6 Simulated operating schedule of the system operations in part load with restriction to the total heat demand

Table 3 presents the results of the simulations of the numerical model for two cases (part load and full load operation) with restriction to the demand of heat for sanitary hot water and space heating. The first column of Table 3 shows the output of the objective function of the optimization model, which is the final minimized cost. The final minimized cost is the overall economic cost of the electrical energy produced and the fuel energy consumed during the system operation for a 24 h simulation time. The positive value of the final minimized cost means that the economic value of the total consumed energy is greater than the economic value of the total produced electrical energy. Since the fuel consumed due to the system operation is the cost for the user, it is desirable to maintain the lower positive value of the final minimized cost. If the final minimized cost was negative, it would mean the user would earn money with the corresponding system operation mode. This can happen because the user does not have to buy electricity at state prices and can obtain the subsidies for the production of electricity. The next two columns in Table 3 represent the total produced electric energy and the total consumed fuel energy for a 24h-simulation time. As a result, it can be concluded that this simulation operation in full load has led to the lower economic costs than the operation in part load.

Table 3 Comparison of the simulation results of the numerical model in part load and full load operation with restriction to the total heat demand profile

	final minimized cost [EUR]	**total produced electric energy [kWh]**	**total consumed fuel energy [kWh]**
full load	2.41	17.77	122.03
part load	3.03	17.13	128.70

Results only for SHW

a) Operation in full load

Figure 7 represents results of the numerical model simulation of the system operation in full load with respect to the heat demand for sanitary hot water (orange line). The SHW profile is characterized by a few zero heat power demand values (i.e. due to no need for hot water from customers during the night). This results in a different operational schedule of the system than for the heat profile with the constant demand of heat. Only, at the 12th time interval, so after 22 000 s (more than 6 hours) should the system start operating according to the simulation. After that time, the buffer vessel capacity reached its minimum due to the consumption of heat from BV and heat losses. For the total considered simulation time (24 h), nine starts of the system correspond to the black bars on Figure 7. The number of starts in this simulation is lower than for the simulation from the section above, where the heat demand was greater than zero for each iteration time and the power values of demanded heat were different.

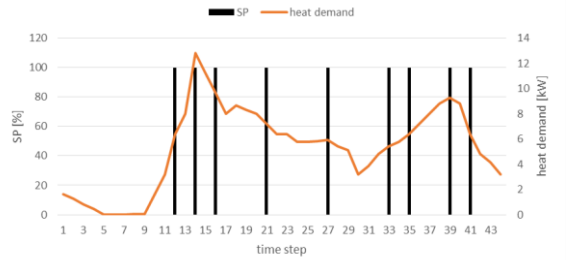

Figure 7 Simulated operating schedule of the system operations in full load with restriction to the SHW heat demand

b) Operation in part load

Figure 8 represents the simulation results of the numerical model of the system operation in part load with respect to heat for sanitary hot water (orange line). As expected, similarly to the simulation of full load operation with the same heat demand, from Figure 8, it can be seen that the system should start operating only after 11 steps of iteration. The number of starts of the system according to this simulation should be 11 to comply with the heat demand and it is greater than for the operation at full load.

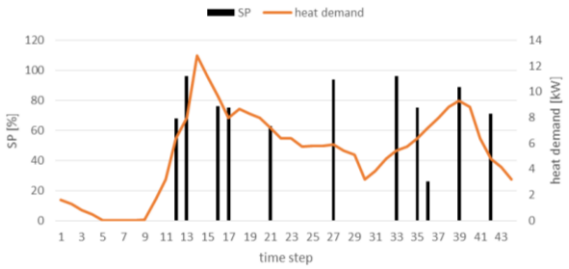

Figure 8 Simulated operating schedule of the system operations in part load with restriction to the SHW heat demand

Table 4 represents the comparison of the simulation results of the numerical model of the system operating in full load and in part load with respect to the demand of heat for sanitary hot water. Similarly to Table 3, the first column of represents values of the minimized cost of operating the system in full load and part load. The second and the third columns show the total produced electric energy and consumed fuel energy during the operation scheme presented on Figure 7 and Figure 8, respectively. As in the case of the simulation results from section above, operation in full load is more economically efficient to comply with the defined heat demand. However, the difference in values of the final minimized cost is not significant. The benefit of operation in full load, in this case, is smaller than for the case described in the previous paragraph because, according to the simulation results, the difference in the number of the system starts is smaller in this case.

Table 4 Comparison of the simulation results of the numerical model in part load and full load operation

	final minimized cost [EUR]	**total produced electric energy [kWh]**	**total consumed fuel energy [kWh]**
full load	2.06	18.00	117.64
part load	2.49	12.58	98.73

4. CONCLUSIONS

Along with this work, the numerical model of the system operation was developed in Python. The result of the numerical model is the objective function that translates the meaning of the economical overall costs of operating the system (micro-CHP and buffer vessel) to comply with two distinguished heat demand profiles. The conclusions from the simulations of the numerical model proved that it is more efficient to operate the system in full load than in part load when the plant is equipped with a buffer vessel of 800 liters and has to comply with the presented heat demand profiles. It means that it is more efficient to start and stop the system more often than to operate at part load. During start and stop, the system produces electricity and heat production less efficiently than in nominal load. The part load operation is as well characterized by smaller efficiency. Operating at full load with the buffer vessel temperature control results in more intermitted operation of the system and causes efficiency losses. However, according to the work presented in this Thesis daily operational cost of the micro-CHP is still smaller at full load.

It is essential to operate micro-CHP in an optimal manner in order to decrease the running economical costs. When running micro-CHP efficiently, less energy is consumed and therefore, less fuel, which contributes to fewer

emissions production. The environmental aspects are one of the drivers encouraging the development of micro-CHP in the market. Due to EU stricter regulations, governments have to find a way to produce energy more efficiently.

In terms of economic aspects, micro-CHP fed with the natural gas is especially attractive when having the prices of NG almost five times lower than electricity prices (like in Germany in 2016). This allows maintaining the daily cost of the production of heat and electricity in the range of a few euros when complying with the discussed heat demand profiles.

7. REFERENCES

1. Houwing M., Ajah A. N., Heijnen P. W., Bouwmans I., Herder P. M. Uncertainties in the design and operation of distributed energy resources: The case of micro-CHP systems. Energy. 2008;33(10):p.1518–1536..

2. Nascimento M. A. R., Rodrigues L., Santos E. C., Gomes E. B., Dias F. L. G., Velásques E.I.G., Carrillo R. A. M. Benini D. E., editor. Progress in Gas Turbine Performance. InTech; chapter 5; ISBN 978-953-51-1166-5. 2013. p.109

3. Chicco G., Mancarella P. Distributed multi-generation: A comprehensive view. Vol. 13, Renewable and Sustainable Energy Reviews. 2009. p. 535–551.

4. Chicco G, Mancarella P. From cogeneration to trigeneration: Profitable alternatives in a competitive market. IEEE Trans Energy Convers. 2006;21(1):265–72.

5. Cogen Europe (Cogen). Micro-CHP fact sheet the United Kingdom. 2005.

6. CODE2 - Cogeneration Observatory and Dissemination Europe. European cogeneration roadmap. 2015;(January).

7. Darrow K., Tidball R., Wang J., Hampson A. Catalog of CHP Technologies. 2017. Available from: http://www.epa.gov/chp/documents/catalog_chptech_full.pdf ; p.1-6; [cited 2017-09-08]

8. Elhadidy M. A. Performance evaluation of hybrid (wind/solar/diesel) power systems. Renewable Energy. 2002;26(3):p.401–413.

9. Caliano M., Bianco N., Graditi G., Mongibello L. Economic optimization of a residential micro-CHP system considering different operation strategies. Appl Therm Eng. 2016;101:p.592–600.

10. Magnani S., Pezzola L., Danti P. Design optimization of a heat thermal storage coupled with a micro-CHP for a residential case study. ScienceDirect. Energy Procedia. 2016;101:p.830–837.

11. Ondeck A., Edgar T. F., Baldea M. A multi-scale framework for simultaneous optimization of the design and operating strategy of residential CHP systems. Appl Energy. 2017;205:p.1499–1511.

12. Camporeale S. M., Fortunato B., Torresi M., Turi F., Pantaleo A.M., Pellerano A. Part Load Performance and Operating Strategies of a Natural Gas-Biomass Dual Fueled Microturbine for Combined Heat and Power Generation. J Eng Gas Turbines Power. 2015;137(12):p.121-401. Available from: http://gasturbinespower.asmedigitalcollection.asme.org/article.aspx?doi=10.1115/1.4030499

13. Minciuc E., Le Corre O., Athanasovici V., Tazerout M., Bitir I.. Thermodynamic analysis of tri-generation with absorption chilling machine. Vol. 23, Applied Thermal Engineering. 2003. p. 1391–1405.